

## Influence of the $sp^2$ content on boron doped diamond electrodes applied in the textile dye electrooxidation

F.L. Migliorini<sup>a</sup>, M.D. Alegre<sup>a</sup>, S.A. Alves<sup>b</sup>, M.R.V. Lanza<sup>b</sup>, M.R. Baldan<sup>a</sup> and N.G. Ferreira<sup>a</sup>

<sup>a</sup> Instituto Nacional de Pesquisas Espaciais, São José dos Campos, Brasil.

<sup>b</sup> Instituto de Química de São Carlos, Universidade de São Paulo, São Carlos, Brasil.

This work presents the production, and the characterization of Boron-doped diamond (BDD) films deposited on Titanium (Ti) substrate (BDD/Ti) with different  $sp^2$  contents. The electrooxidation of the dye Reactive Orange 16 (RO16) is studied systematically considering the  $sp^2$  bonds influence. The results for the dye electrochemical degradations were investigated by spectroscopic techniques UV/VIS analysis, Total Organic Carbon (TOC), and High Performance Liquid Chromatography (HPLC). The BDD electrode with the lowest percentage of  $CH_4$  showed the best efficiency for the aromaticity reduction, the reduction of solution color and in the analysis of the TOC. This performance was associated to its best diamond purity. This study also demonstrated that there is a compromise between the conductivity of the films and the increase of bonds  $sp^2$  type.

### Introduction

Industrial pollutants are known due to their toxicity and persistence in the environment. Several methods have been studied to eliminate or decrease the toxic effects of these compounds [1]. Among these methods, EAOP (electrochemical advanced oxidative processes) have been used with success and they are based on the *in situ* electrogeneration of highly reactive hydroxyl radical ( $\bullet OH$ ). Thus, it is a promising environmental technique [2].

The major problem is the chosen of anode material which should be stable, resistant and efficient. BDD (boron diamond doped) anodes are used with success on the organic compound treatment and the mechanism involves hydroxyl radical generation physically adsorbed. The film can be grown up on several substrates but titanium substrate gives mechanical resistance to industrial application [3–5].

There are various industrial effluents but dyes textile are potentially genotoxic on aquatic biota and on humans [6]. This type of effluent is characterized by extreme fluctuations in many parameters such as chemical oxygen demand (COD), biochemical oxygen demand (BOD), pH, color and salinity. Recalcitrant organic, colored, toxicant, surfactant and chlorinated compounds and salts are the main pollutants in textile effluents [7]. Dyes are indeed refractory to microbial degradation because of their substitution groups such as azo, nitro or sulpho groups. The majority of these compounds consumed at industrial scale are azo ( $-N=N-$ ) derivatives. They have a wide range of applications in textile, pharmaceutical and cosmetic industries, and are also used in food, paper, leather and paints. However, some azo dyes can show toxic effects, especially carcinogenic and mutagenic events [8].

## Experimental Procedure

### Preparation and Characterization of BDD/Ti Electrodes

The BDD electrode was grown on Ti substrate by hot filament chemical vapor deposition (HFCVD) technique. The deposition of diamond on titanium has a singular characteristic attributed to the strong stress formation between the film and the substrate, which arises from extrinsic and intrinsic factors. In this sense, some pre-treatments on the substrate surface are required to decrease the stress and to increase the nucleation rate [20-22]. Among them, the mechanical incision is effective to increase the titanium surface area and roughness improving the mechanical anchoring of the film. This incision was made in air abrasion with glass beads. The treated surface ensures the best adhesion of the diamond coating due to its higher effective area for the film deposition. The BDD/Ti films were grown on titanium substrate of 2.5x2.5x0.5 mm at CH<sub>4</sub> additions of 1, 2, 6 and 10 sccm diluted in H<sub>2</sub> for a total flow rate of 200 sccm. The temperature and the pressure inside chamber reactor were kept at 650 °C and at 40 Torr, respectively. The sample was grown for 16 h. The doping control was obtained from an additional H<sub>2</sub> gas flux passing through a bubbler containing a solution of B<sub>2</sub>O<sub>3</sub> dissolved in CH<sub>3</sub>OH with the B/C ratio of 15.000 ppm. This additional hydrogen flow into the reactor was controlled by a rotameter which was maintained at 40 sccm (standard centimeter cubic per minute). This doping level corresponds to 10<sup>20</sup> cm<sup>-3</sup> evaluated by Mott Schottky measurements. The top view SEM images of BDD/Ti films were obtained from a Jeol equipment JSM-5310. The quality of BDD/Ti films were analyzed from Micro-Raman spectra recorded by a Renishaw microscope system 2000 in backscattering configuration. The diamond patterns in addition to hydrides and titanium carbides phases were monitored by grazing incident X-ray diffraction (GIXRD) using a Philips X'Pert diffractometer.

### Condition Monitoring and Degradation of Dye RO16

The electrochemical degradation of RO16 azo-dye solution supplied by Aldrich (~50% m/m) was performed in a polypropylene home-made single cell with capacity of 0.45 L. The BDD/Ti working electrode (~ 4.15 cm<sup>2</sup> of the geometric area) was located at the bottom of the cell. A platinum screen, 2 cm in diameter, was used as a counter electrode and a commercial Ag/AgCl electrode (3.0 mol L<sup>-1</sup> KCl solutions) was used as the reference electrode. All the degradation assays were performed at 25 °C and at constant stirring. The electrooxidation experiments were performed at current density of 50 mA cm<sup>-2</sup> using 150 mg L<sup>-1</sup> of the RO16 azo-dye and K<sub>2</sub>SO<sub>4</sub> 0.1 mol L<sup>-1</sup> (pH= 10), in a total treatment time of 90 min. All electrochemical measurements were carried out using a potentiostat/galvanostat AUTOLAB model PGSTAT 302 (Eco Chimie) coupled with a BRTS-10A current booster, controlled by the GPES software.

### Instrumentation and analytical conditions

Concentration analyses of RO16 azo-dye were carried out with high pressure liquid chromatography (HPLC) Shimadzu 20A with UV/Visivel detector SPD-20A. The stationary phase used was a reverse fase column (C<sub>18</sub> Varian Pursuit 5 250x4.6 mm) while the mobile fase was the ammonium acetate/methanol with proportion of 70:30 with flow of 0.8 mL min<sup>-1</sup> for wavelength of the 249 nm at 40 °C. The ion chromatograph Pro 850 Metrohm was used to detect and to quantify the inorganic ions

formed during the electrolysis. A column A Supp 5 with mobile phase of  $3.2 \times 10^{-3}$  mol L<sup>-1</sup> of sodium carbonate and  $1.0 \times 10^{-3}$  mol L<sup>-1</sup> of sodium bicarbonate (J.T Baker) was used with flow of  $0.7$  mL min<sup>-1</sup> and a conductivity detector. The Total Organic Carbon (TOC-VCPN Shimadzu) technique was employed to determine the removed organic material. The UV-Vis spectra were recorded in Varian Cary 50 Scan spectrometer in the range from 300 to 600 nm. The maximum absorption used to calculate the concentration by UV/Vis was at wavelength of 388 nm.

## Results and discussion

### Morphological and Structural Characterization of Diamond Electrode

The top view SEM images of one sample set doped with B/C ratio of 15000 ppm is shown in Fig. 1 (A-D), which correspond to a general view of the electrodes surface morphologies grown with 1, 2, 6 and 10 sccm of CH<sub>4</sub>, respectively. BDD images show continuous and homogeneous films covering the entire substrates. Considering the challenge to grow diamond on Ti, the films are very adherent, without cracks or delaminations. The BDD morphology is associated to the microcrystalline grains randomly oriented with dominant (111) direction. As expected, the microcrystalline grain agglomerates as a function of CH<sub>4</sub> addition in the gaseous mixture. This transition can be directly observed when we compare Fig. 1 A with Fig. 1 C.

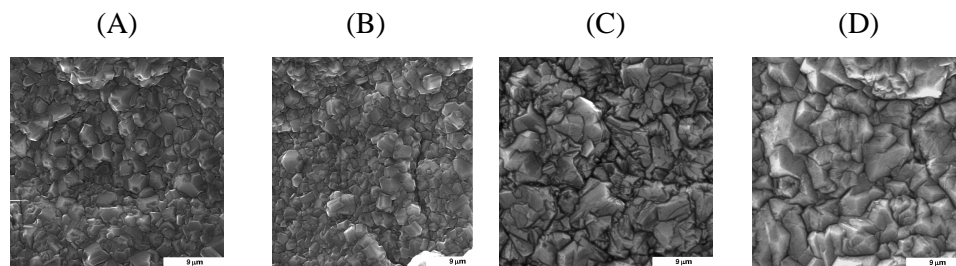


Figure 1: Scanning electron micrographs (SEM) of diamond films grown on titanium substrate with 15000 ppm with different concentrations of CH<sub>4</sub>. A) 1 sccm, B) 2 sccm, C) 6 sccm and D) 10 sccm of the CH<sub>4</sub>.

The film quality investigated by Raman spectroscopy is shown in Fig. 2 (A). The presence of a Raman peak around  $1332$  cm<sup>-1</sup> was verified, which corresponds to the diamond first-order phonon vibration. We also observed an emergent band at  $1230$  cm<sup>-1</sup>, characteristic of the boron doped diamond films, which is attributed to the induced disorder in the diamond structure due to the boron incorporation [9-11]. This band increases significantly by increasing the doping level associated to a drastic reduction in the diamond peak. This process is assigned to the relaxation of selection rule  $k = 0$  of Raman scattering due to the presence of a very high concentration of boron in the diamond lattice [11]. The appearance of a band around  $500$  cm<sup>-1</sup> is also observed, attributed to the vibration of boron pairs in diamond lattice [11]. More recently, Niu et al. [12] have discussed the electronic and vibrational properties of heavily doped BDD and have concluded that the bands at  $500$  and  $1230$  cm<sup>-1</sup> are both superposed including not only C vibrations but also B-B and B-C vibrations, respectively. The G band around  $1580$  cm<sup>-1</sup> is also present, attributed to graphitic phases. The band around  $1580$  cm<sup>-1</sup>

becomes more pronounced for films grown with 6 and 10 sccm of CH<sub>4</sub>, confirming the sp<sup>2</sup> incorporation increase in these films.

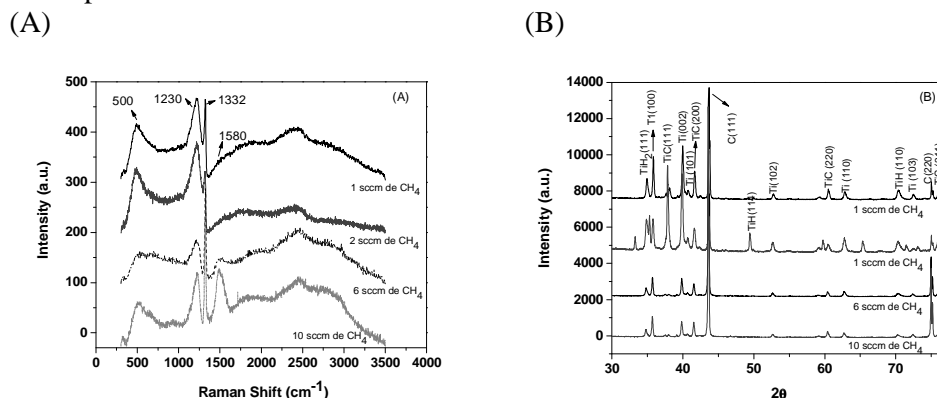


Figure 2: (A) Raman Spectra of diamond films grown at a different CH<sub>4</sub> content. (B) X-ray diffraction of diamond films grown at a different CH<sub>4</sub> content.

X-ray diffraction results are shown in Fig.2 (B) and were collected in the incidence angle of 1° over the range from 30° to 80°. For this geometry, the grazing incident X-ray diffraction (GIXRD), the oblique angle to the penetration depth of the X-rays is largely reduced, facilitating the identification of different phases present in the BDD films. Another feature of this method is the illumination of a large sample area allowing the detection of thin layers that may be present in the film/substrate interface such as carbides (TiC) and hydrides (TiH). For all sample sets studied the patterns clearly depict the 2θ peaks at 75.5° and 44° corresponding to the (111) and the (220) diamond diffraction planes, respectively assuring the material crystallinity. The diffractograms also show the formation of TiC phase related to the peaks <111>, <200>, <220> and <311>, the TiH phase related to peaks <114> and <110>, the TiH<sub>2</sub> phase related to <111>, and the Ti phase related to <100>, <002>, <101>, <102>, <110> and <103> [9]. As previously discussed, the growth of diamond films on Ti substrate is a challenge. During the deposition of diamond, carbon and hydrogen present in the gas atmosphere diffuse into the titanium matrix forming TiH and TiC phases. The formation of these phases is directly related to the growth conditions. Thus, it is very important to optimize the experimental parameters to grow diamond films on titanium substrates with good quality and adherence.

### Electrochemical degradation of the RO16 dye with BDD/Ti electrodes

#### UV/VIS analysis

To evaluate the electrodes efficiencies an important parameter is the color removal during the degradation process of the species. The RO16 dye presents two bands of absorption in the visible spectrum. The first, at around 390 nm, may be associated with the π-π\* transitions of the aromatic rings and the other, at around 500 nm, is attributed to the n-π\* transitions of the chromophoric (-N=N-) azo group, present in the RO16 molecule. Thus, the color removal of the solution containing the dye, resulting from the reaction of the chromophore groups of the molecule, can be monitored from the intensity variation of these main absorption bands. Figure 3 shows the absorption spectra for the electrode with a lower percentage of CH<sub>4</sub> from 300 to 600

nm for the RO16 solution electrolyzed at current density of  $100 \text{ mA cm}^{-2}$ , respectively, for seven electrolysis times varying 10 to 90 min.

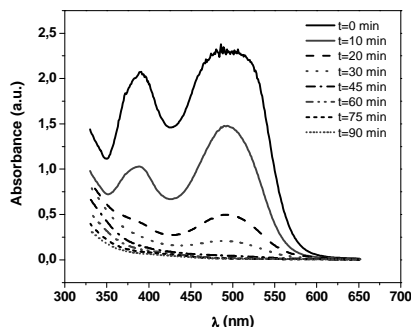


Figure 3: Absorption spectra for the RO16 at  $100 \text{ mA cm}^{-2}$  with the diamond films grown on titanium substrate with a lower percentage of  $\text{CH}_4$  (1 sccm).

For all electrodes, it is possible to observe an extreme reduction in the intensities of the two azo-dye absorbance bands as a function of the electrolysis time, since at the end of the 90 min these two bands are almost totally vanished. This states the great efficiency of the electrochemical treatment for the color reduction by using BDD/Ti electrodes. It is interesting to highlight that all electrodes were efficient in the rupture of the azo group in the aromatic bonds of the azo-dye molecule. The electrode with a lower percentage of  $\text{CH}_4$  was more efficient for aromaticity reduction and group fracture when compared with the other electrodes. This electrode removed completely the color just after 10 min while a similar result were observed for the others electrode only after 20 min to the electrode with 2 sccm de  $\text{CH}_4$  and 60 min to the electrode with 10 sccm de  $\text{CH}_4$ , the electrode with 6 sccm de  $\text{CH}_4$  even after 90 min of treatment the color remained. This trend in the results can be justified on the ground that the electrode with less concentration of  $\text{CH}_4$  can be more organized in structural terms, and mostly for the best quality of diamond deposited. With increasing concentration of  $\text{CH}_4$  in the gas mixture leads to an increase of defects with inclusion of impurities, mainly  $\text{sp}^2$  type. So, an intrinsic consequence of the addition of  $\text{CH}_4$  in the gas mixture is increased participation of type  $\text{sp}^2$  carbon in the diamond films. As we can see, this type of participation of  $\text{sp}^2$  carbon in the films proved detrimental to the concentration of 6 sccm, because there was a decrease in the degradation efficiency. From the concentration of 10 sccm was an improvement in the efficiency degradation of the dye, but the increase in conductivity with the participation of  $\text{sp}^2$  failed to overcome the result with the electrode of higher purity diamond.

### TOC Measurements

The total organic carbon (TOC) analysis was performed. TOC is a strong indicative of the efficiency of electrochemical process to mineralize organic matter present on the colorant solution. The electrode with a lower percentage of  $\text{CH}_4$  presented a higher efficiency for the TOC reduction than that the other electrodes. The electrode with 1 sccm of the  $\text{CH}_4$  propitiated about 30% TOC elimination against about 25, 13 and 20% removal for the electrodes with 2, 6 and 10 sccm of the  $\text{CH}_4$ , respectively. The electrochemical treatment of the RO16 azo-dye solutions with BDD/Ti electrodes containing different levels of the  $\text{CH}_4$  presented a significant TOC removal, in addition to the complete color removal.

### HPLC Qualitative Detection

The aromatic intermediates produced during each electrochemical treatment containing RO16 dye were detected by high performance liquid chromatography (HPLC) using a wavelength of 254 nm. The appearance of chromatographic signal at 254 nm is related to the  $\pi$ - $\pi^*$  transition of the conjugated systems, such as aromatic compounds that make up the solution of the RO16 dye. Figure 4 shows the chromatograms of solutions containing RO16 dye untreated (1) and the solutions after electrolysis at current density of  $100 \text{ mA cm}^{-2}$ : 30 min (2) and 90 min (3), for the electrode with the lowest percentage of  $\text{CH}_4$ .

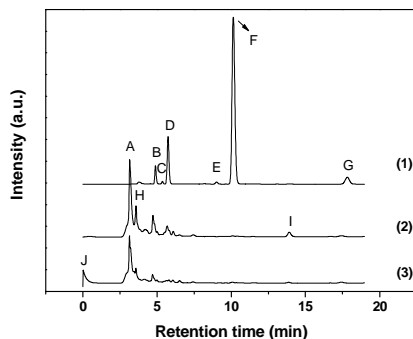


Figure 4: Chromatograms of RO16 dye samples obtained with a current density of  $100 \text{ mA cm}^{-2}$  with the electrode the lowest percentage of  $\text{CH}_4$ , for the times: (1) 0 min, (2) 30 min and (3) 90 min.

For the untreated dye solution (chromatogram A), at least seven aromatic compounds appeared, with different polarities and retention times that must be directly associated with the dye RO16. After the electrochemical treatment at  $100 \text{ mA cm}^{-2}$  (chromatograms of 30 and 90 min), the peaks disappeared, indicating a considerable reduction of the aromatic compounds. One can observe the appearance of other peaks with lower retention time, which implies the presence of more polar compounds with characteristics that the dye study. Comparing the results we can observe the same trend for all electrodes, but the electrode with the lowest percentage of  $\text{CH}_4$  showed a lower amount of peaks and lower retention time, which would imply the presence of more polar compounds that present smaller aromatic chain. This reduction in the aromaticity of RO16 dye solution led to the possible formation of compounds of the aliphatic chain. From an environmental standpoint these compounds are very important because they tend to be biodegradable. This result confirms that the film with improved purity of diamond is most suitable for this type of application.

### **Conclusion**

This study showed an extreme reduction in the intensities of the two azo-dye absorbance bands for all the electrodes studied. However, the electrode with the lowest percentage of  $\text{CH}_4$  presented the best efficiency in the degradation process. This behavior may be attributed to its semiconductor character, and by the better quality of diamond deposited confirming that the diamond with smaller amounts of impurities is most suitable for this type of application. This result may be associated with the aromaticity reduction, the reduction of solution color and by TOC analysis.

### Acknowledgments

The authors gratefully acknowledge the financial support provided by FAPESP (2010/18462-2), CNPq and CAPES.

### References

1. V.K. Gupta, R. Jain, A. Nayak, S. Agarwal, M. Shrivastava, *Materials Science and Engineering: C*, **31**, 1062–1067 (2011).
2. C.A. Martínez-Huitle, S. Ferro, *Chemical Society Reviews*, **35**, 1324–1340 (2006).
3. Z. Frontistis, C. Brebou, D. Venieri, D. Mantzavinos, A. Katsaounis, *Journal of Chemical Technology and Biotechnology*, **86**, 1233–1236 (2011).
4. J.R. Domínguez, T. González, P. Palo, *Chemical Engineering Journal*, **162** (2010) 1012–1018.
5. A.M. Polcaro, M. Mascia, S. Palmas, A. Vacca, *Electrochimica Acta*, 49649–656 (2004).
6. S. Kobylewski, M.F. Jacobson, *International Journal of Occupational and Environmental Health*, **18**, 220–246 (2012).
7. S. Ahmed, M.G. Rasul, W.N. Martens, *Water Air & Soil Pollution*, **215**, 3–29 (2011).
8. E. Guivarch, S. Trevin, C. Lahitte, *Environmental Chemistry Letters*, 38–44 (2003).
9. J.W. Ager, W. Walukiewicz, M. McCluskey, M.A. Plano, M.I. Landstrass, *Applied Physics Letters*, **66**, 616-618 (1995).
10. R.J Zhang, S.T. Lee, Y.W. Lam, *Diamond and Related Materials*, **5**, 1288-1294 (1996).
11. P.W. May, W.J. Ludlow, M. Hannaway, P.J. Heard, J.A. Smith, K.N. Rosser, *Diamond and Related Materials*, **17**, 105-117 (2008).
12. L. Niu J-Q. Zhu, X. Han, M-L. Tan Gao, W, S-Y. Du, *Physics Letters*, **373**, 2494-500 (2009).